Chapter VIII

Global optimization strategies in ray tracing deflection tomography: Accuracy and possibilities for evaluating the gradient-index in crystalline lenses

Coauthors of the study are: Adrian Glasser, Chris Clark and Susana Marcos.

Adrian Glasser and Chris Clark form the Optometry College of Houston and Susana Marcos from the Instituto de Óptica, Madrid.

The contribution of Sergio Barbero to the study was to implement the optimization strategy to the tomography problem, perform the experimental measurements in the commercial lens, analysis of data and discussion on results.

RESUMEN

OBJETIVOS: Desarrollo y estudio de una técnica no destructiva, *in vitro,* para medir la estructura de gradiente de índice (GRIN) presente en el cristalino. La técnica esta basada en un montaje experimental óptico basado en el registro de la deflexión de la luz y la aplicación de algoritmos de optimización global. Las posibilidades y precisión de la técnica se han estudiado usando como calibración una lente de GRIN conocido. **MÉTODOS:** El montaje experimental esta compuesto de un scanner, dos cámaras CCD y un contenedor para la lente. Un haz de 0.5 mm de diámetro es escaneado paralelo al eje óptico por diferentes posiciones sobre la lente y los rayos refractados son registrados por las cámaras. Las pendientes de las trayectorias de los rayos refractados son los datos experimentales usados por el algoritmo de optimización. El algoritmo de optimización usa métodos de búsqueda globales, implementados en un programa de diseño óptico (Zemax). A partir de un modelo a priori de la estructura GRIN, el algoritmo de optimización busca la solución que mejor se ajusta a los datos experimentales. El procedimiento completo se ha evaluado en una lente comercial (GBX-25-40, GRADIUM., LightPath Technologies) con un perfil de GRIN conocido descrito por un polinomio de 11^{th} orden. Asimismo se estudio como el nivel de precisión se propaga al análisis óptico de la lente en términos de aberración de onda.

RESULTADOS: La precisión "teórica" de la técnica, esto es sin presencia de errores experimentales, en la reconstrucción del GRIN esta limitada por un error absoluto medio de 0.0024±0.0022 respecto del valor nominal del GRIN. Con los datos experimentales reales el error se incrementa hasta 0.041±0.017. Estos errores se manifiestan en los coeficientes de la aberración de onda con unas diferencias de 0.00021 µm, sin tener en cuenta los errores experimentales, y 0.014621 µm teniéndolos en cuenta. **CONCLUSIONES:** En ausencia de errores experimentales, los algoritmos de optimización global son lo suficientemente robustos incluso en modelos con un número elevado de parámetros. Sin embargo con los datos experimentales los errores en la reconstrucción del GRIN se incrementan significativamente debido a la naturaleza *ill-conditioned* de la optimización. Para una futura implementación de la presente técnica en cristalinos reales, se deberá reducir los errores experimentales y usar modelos realistas de la estructura GRIN en el cristalino.

ABSTRACT

PURPOSE: To study the use of an *in vitro* non-destructive technique based on an optical experimental set up with ray refracted recording and use of global optimization algorithms to evaluate the gradient index structure presented in crystalline lens. The possibilities and accuracy of the technique is studied by evaluating the reconstruction of the GRIN distribution of a glass lens with known GRIN profile. **METHODS:** The experimental method uses a laser scanning system, two CCD cameras, and a glass chamber in which the lens is placed. A 0.5 mm diameter laser beam is scanned parallel to the optical axis at multiple different positions over the lens, and the refracted rays trajectories are recorded by the cameras. The measured slopes of the ray trajectories are the experimental data used for the optimization procedure. This procedure uses global search optimization routines, implemented in an optical design program (Zemax). The method starts with a priori assumptions about the GRIN model and uses the experimental data to find the best solution for the unknown GRIN distribution. The global procedure was tested on a commercial gradient index lens (GBX-25-40, GRADIUM., LightPath Technologies) with a known GRIN profile described by an 11^{th} order polynomial. The effect of the accuracy in the GRIN reconstruction on the optical evaluation in terms of wave aberration analysis was evaluated. **RESULTS:** The theoretical accuracy of the optimization routine on the GRIN profile reconstruction, excluding experimental error, is limited by a mean absolute error of 0.0024±0.0022 with respect the nominal profile. However the error increases, for the real experimental data, to 0.041±0.017. These errors result in a mean standard deviation error of the coefficients of the wave aberration of 0.00021 μm and 0.014621 μm with and without experimental error respectively. **CONCLUSIONS:** Global optimization is a robust procedure with models involving a large number of parameters in the absence of experimental errors. However with real experimental data, the error in the reconstruction increases significantly due to the *ill-conditioned* nature of the optimization. Practical implementation of this technique in a real crystalline lens will require a significant reduction of experimental errors and realistic assumptions of the actual GRIN distribution.

1. Introduction

In previous chapters it has been shown how combined measurements of corneal and total aberrations provide an estimation of the contribution of internal optics in different situations. By internal optics we referred to the contribution of the posterior corneal surface and, predominantly the crystalline lens. The crystalline lens is composed of an external epithelial layer and a nucleus and cortex made of fibre layers (fibre cells which have lost their nuclei) all within an elastic capsule. The nucleus and cortex have a non-uniform gradient index structure. Thus, to understand the sources of aberrations found in crystalline lens it is not only necessary to estimate the shape of the anterior and posterior lens surfaces, but also to evaluate its gradient index structure.

1.1 The crystalline lens as a gradient index structure.

The crystalline lens optical properties are determined by the knowledge of the lens surface shape and the refractive index distribution, which is usually referred to as the gradient index or GRIN (GRadient INdex). Equivalent refractive index, a single value representing the overall contribution of the refractive index, has been used as a simplification for understanding overall refracting power of the crystalline lens. It is also useful to determine the importance of the GRIN structure by means of direct comparison with the same lens with an equivalent refractive index. It has been pointed out that in vertebrate, and specifically human crystalline lenses, a GRIN with refractive index higher in the nucleus than in the periphery, plays an important role in balancing the positive spherical aberration[1]. A GRIN also reduces the index difference between the lens surface and the humours surrounding the lens, thus reducing scattering and reflecting effects in lens surfaces[2]. Knowledge of the structure of the GRINs is essential to understand the role of the crystalline in the imaging properties of the eye, as well as to understand basic optical properties of the eye, such as in accommodation or presbyopia. Further, refractive index is closely related to distribution of proteins[3] and so understanding the GRIN structure of a lens may help to understand the relationship

between the optical properties and biochemistry of the lens.

The modelling of the refractive index of the lens should represent the real refractive properties as close as possible to the real physiology. Ideally this is achieved by the knowledge of a scalar field: u(x,y,z) that represents values of refractive index for the different spatial coordinates (x,y,z). Because of the complex physiological structure of the lens, u(x,y,z) can not be evaluated by a simple analytical function. Therefore some approximations must be used in order to represent u(x,y,z) with enough precision but with a manageable number of parameters, that allow to perform some basic calculations such as those can be achieved with ray tracing algorithms.

Current models for the GRIN, u(x,y,z), are either too general, as general series expansion with the only restriction of rotational symmetry about the optical axis or too simplified as bi-elliptical models[4]. The first type of models requires a large amount of parameters while the second type requires only few number.

1.2 GRIN measurement.

Different techniques have been used to retrieve information on the GRIN in vertebrate lenses. All of them can be divided in two main type, destructive, i.e. those in which the lens is bisected and non-destructive, i.e. those in which the intact lens is considered. Destructive techniques include evaluating slices with conventional refractometers[5], interferometric techniques[6], or by linking protein concentration with refractive index by microradiography[7]. Non-destructive techniques include using tomography techniques, such as in vitro nuclear magnetic resonance (NMR) micro-imaging[8] (assuming linear relation between protein concentration and index of refraction) or techniques using information of the optical path of light as it passes through the lens (deflection tomography). Some tomography approaches use regression techniques in fitting to a known model of the GRIN information on either spherical aberration in emmetropic eyes[9] or lens optical power[10]. However, the most typical methods use information of laser beam deflection traversing the lens recorded in vivo by Scheimpflug images[11] or in vitro[12-14].

1.3 Goals of the present work

In this work we present a tomography method based on global optimization and we test the possibilities and the theoretical accuracy of the methodology to be used in retrieving complex GRIN profiles such as the GRIN of the human crystalline lens. For this purpose we test the technique in a commercial glass lens where the GRIN profile is known. In addition we show how the error in the GRIN reconstruction is propagated in the estimation of the optical properties of the lens in terms of its wave aberration.

2. Methods

We consider a tomography technique which involves digitization of laser beams passing through multiple selected planes of the lens. This is based on measurements of the deflection of laser ray beams traversing lenses in vitro. It uses an iterative regression with a previous assumed function for the GRIN, that combines local damped least squares routines with global search strategies based on genetic algorithms. We test the accuracy of this approach by using a commercial glass GRIN lens with a known profile given by a tenth order power series polynomial.

2.1 Theoretical background

Physics of the tomography technique

Figure VIII.1 represents the ray paths of a series of parallel laser rays passing into a bi-convex lens.

In geometrical optics the incoming set of parallel laser rays is described by a constant plano wavefront, with the relationship between ray directions ($\boldsymbol{r}$) and wavefront ($\boldsymbol{W}$) being determined by the eikonal equation:

$$\boldsymbol{n} * \boldsymbol{r} = \nabla \boldsymbol{W} \qquad \textbf{(1)}$$

where n is the refractive index

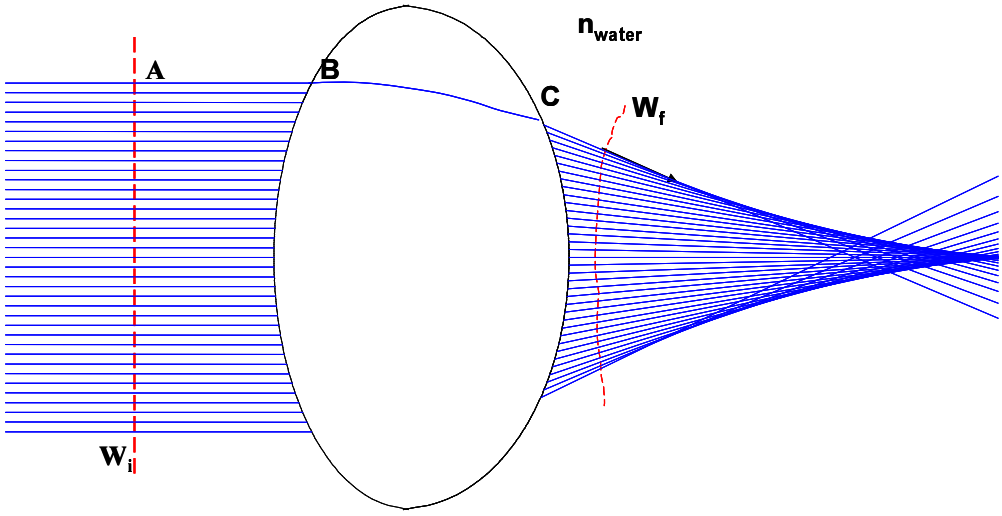

Figure VIII.1: Geometrical optics representation of experimental ray tracing through a bi-convex lens. W_i represents the incoming wavefront and W_f the outgoing wavefront.

If A is a point of the incoming wavefront that intersects the lens at the point B, travels trough the GRIN lens by a path BC, given by Fermat's principle, then the ray vector at C is obtained by knowing the wave-front and using equation (1).

The wavefront is determined by the optical path and starting at point A the wavefront at C is given by optical path length between A and C:

$$W_c = AB * n + \int_B^C u(s)ds \qquad (2)$$

where s is the parametric variable of the curve described by the ray inside the lens and u(s) is the refractive index as a function of s.

In two dimensions, equation (1) is expressed as:

$$\frac{\partial W}{\partial z} = n * \cos(\alpha) \qquad (3)$$

where α is the slope of the ray in the optical axis direction. The solution to (3) is a function of α and a constant, because in the derivative of (3) the constant is cancelled.

$$W_c = f(\alpha) + cte \qquad (4)$$

Joining (2) and (4) we have the following equation that defines the tomography problem:

$$\int_B^C u(s)ds + cte = f(\alpha) + AB * n \qquad (5)$$

where the right side is obtained by from experimental measurements and the left side are the underlying magnitudes to be evaluate.

Solving the problem to evaluate the GRIN structure of the crystaline lens is reduced to having to estimate the function **u** in the integral of equation (5).

Mathematical solution of the tomography technique

There are different mathematical ways to solve the tomography problem expressed by equation (5). A direct mathematical inversion of the integral in (5) by Fast Fourier Transform (FFT)[15], as first used in the tomography measurement of crystalline lens GRIN by Campbell et al [12], has the inconvenience of requiring a mismatch of refractive index between the boundary of the lens and the immersed medium. Solutions for these restrictions were subsequently proposed, but still having the restriction of radial symmetry[13, 16]. Beliakov and Chan proposed a method to perform the reconstruction with no special symmetry in 2-D[17] that could be extended to rotational symmetric 3-D reconstruction[18]. The complexity of the functional shape of a GRIN, which is expected in a biological tissue such as crystalline lens, limits the mathematical treatment of the inversion problem. A possible method to deal with a complex GRIN consists of direct regression with iterative algorithms of experimental data (e.g. slopes of the refracted rays leaving the crystalline lens recorded by a CCD camera). This strategy is referred to as a modal reconstruction because an *a priori* description for the function that describes the GRIN is required. However it has the powerful benefit of requiring no a priori restrictions in the type of model used and the opportunity to use different models.

The formalism for this technique is established as follows:

If $\mathbf{t_i}$ is the set of experimental measurements – in this case the refracted ray slopes-, $\mathbf{u_i}$ is the set of variables that determine the GRIN function to evaluate.

Then a merit function $\mathbf{A[u_i]}$ is constructed in a way that the variables $\mathbf{u_i}$ are evaluated by minimizing A.

$$A[u_i] = \sum_{i=0}^{N} f_i \qquad f_i = w_i(v_i - t_i)$$

where $\mathbf{v_i}$ are the different values that the merit function takes for the targets $\mathbf{t_i}$, for the different evaluations of $\mathbf{u_i}$, and $\mathbf{w_i}$ are individual weights that can take different values if errors of the experimental measurements are known.

The problem that arises with such a merit function, using only $\mathbf{t_i}$, is that the uniqueness of the solution is not guaranteed for the following reasons:

1) the presence of the arbitrary constant in equation (5),
2) the finite number of experimental measurements $\mathbf{t_i}$,
3) the experimental errors in the measurements of $\mathbf{t_i}$,
4) the complexity of the function u that defines the GRIN. The integral of equation in (5) can take the same value for different shapes for u, with an increasing number of possibilities with increasing complexity of u.

While reason 2) could be minimized by using a large number of measurements, additional assistance must be found to reduce the "solution space" for $\mathbf{A[u_i]}$. In optimization routines this is done by using constraints expressed as a function $\mathbf{B[u_i]}$, to add to the global merit function. Finally, the optimization searches for a solution that minimizes $\mathbf{\Phi[u] = \mathit{A}[u] + \lambda \mathit{B}[u] = 0,}$ where λ is the set of weights to the constraints called Lagrangian multipliers[19]. The success of the optimization depends strongly on the way in which $\mathbf{\Phi}$ is constructed. **A** measures the agreement between the model and the data. If **A** alone is minimized, it could result in an oscillating and "unrealistic" solution. **B** is called the *stabilizing functional* and acts based on a priori expectations of the final solution[19].

In the case of empirical measurements on the crystalline lens we propose the imposition of two constraints:

1) We can suppose that we are able to know, within a determined range of measurement error, the refractive index at the lens surface. Using a reflectometric fibre optic sensor as described by Pierscionek[20] the refractive index measurement error at the surface is ±0.002.

2) Taking into account the "onion layers" structure of the crystalline lens where it is well known that the refractive index falls from the lens nucleus towards the periphery of the cortex, it is reasonable to suppose that the function that describes the GRIN is a continuous and monotonic function with respect to the vector position defining direction from the centre to the periphery of the lens.

2.2 Experimental measurements

The experimental setup has been developed in the College of Optometry (University of Houston), similar to a laser ray tracing technique described previously[21, 22] and using the same principles of the laser ray tracing technique used in chapter II-VI. A 633nm HeNe (5 mW, 0.8 mm diameter) laser beam is scanned with two stepper motors controlling X-Y stage mirrors with a minimum step size of 1µm. The GRIN lens to be evaluated is located in a glass chamber filled with saline with a small amount of powder milk (~1 mg) to allow a sufficient degree of scatter of the laser rays to be observed by two CCD cameras, one from above and the other one from the side. The CCD's are ½ inch square of 512 x 480 pixels. Such configuration allows two bi-dimensional scans in the entrance pupil of the lens. For each of the scans the top and side view images are obtained and processed by image processing software (Optimas Version 6.1, MediaCybernetics). In the image processing, two rectangular regions of interest (ROI's) are selected containing the whole sample of ingoing and outgoing and incoming rays, as seen in figure 2.

The set of pixels that define ray trajectories are found by finding the peak intensity pixel values in each of 50 vertical line profiles within each ROI. Slopes of the rays are then evaluated by linear regression over those 50 positions. Beam centration on the optical axis of the lens was assessed by determining the zero entrance ray position where the slopes of the entrance and exit ray are both close to zero.

2.3 Optimization algorithms

Once the merit function **Φ[u]** is constructed several techniques can be used to minimize it. These methods have been widely used by optical designers in order to improve optical designs from aberrations, or even to optimize GRIN structures in the design of progressive lenses [23].

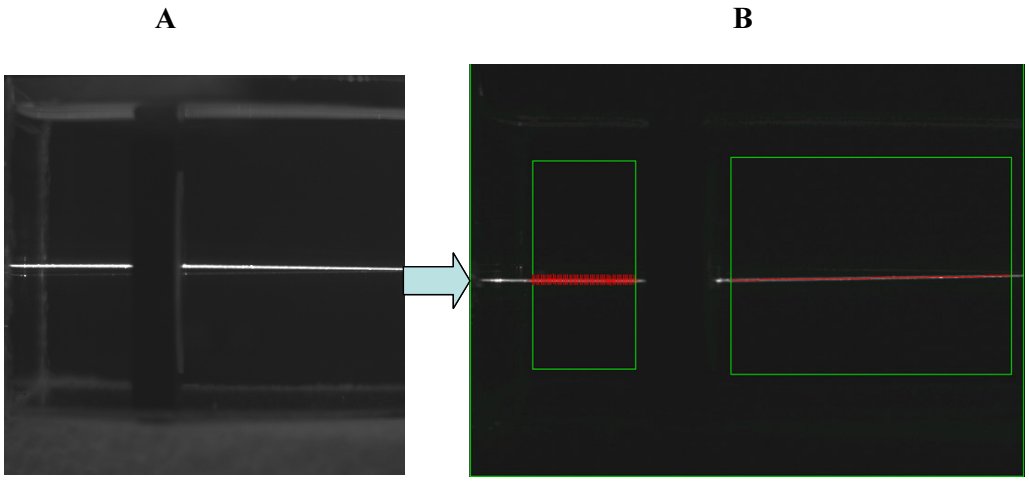

Figure VIII.2: A) Example of image captured by the lateral CCD camera of the experimental set-up. **B)** Green boxes show the region selected for the image processing and red lines show the image profiles where maximum pixels values are evaluated for the ray trajectory detection.

We use these algorithms implemented in an optical design program (Zemax Focus Software, Tucson, AZ) in order to minimize a merit function where the targets $\mathbf{t_i}$ are the experimental slopes measured in the experimental setup described above. The evaluation of $\mathbf{\Phi[u]}$ is performed by computing virtual ray tracing for iterative solutions for **u.** Virtual ray tracing through a GRIN structure uses the Sharma algorithm[24]. In optical design (specifically in ZEMAX software[25]) two different kinds of optimization algorithms are used as will be described below.

Local Optimization: Damped least squares method (DLS)

The most popular optimization algorithm in optical design is based on damped least squares method. This algorithm introduces a "damped" factor in operands of the merit function to assure the convergence of the solution in the least- squares routine[26]. This type of algorithm is called "local" in the sense that, being based on the evaluation of the local gradient of the merit function, it depends on the starting point. Therefore it finds the closest local minimum to that starting point. As a result the global solution is only guaranteed if an appropriate starting point is chosen.

Local optimization has been used by Pozmenoraff et al[9], Al-Ahdali et al[10] and Garner et al [14], this last using ray tracing experimental data, a polynomial GRIN model with four parameters, and using a conjugate directions optimization routine[19].

The principal problem of local algorithms is that in wide solution spaces the solution may be trapped in a local minimum

Global optimization: Genetic Algorithms

Global search methods are used in configurations with complex evaluation functions with complex constraints and dependencies between parameters. All these characteristics are present in our merit function as described above. Genetic algorithms (GA) are optimization techniques inspired by genetic principles. The basic idea is the generation of parallel and scaled random permutations of different combinations of the parameters values, and subsequent "survival" of the family of combinations with a minimum value for the merit function[27]. Therefore these algorithms are expected to avoid the problem of becoming trapped in a local minimum of local optimization. The use of genetic algorithms in tomography has been previously used by Kihm et al [28] to reconstructed density field values from interferometric projections, with promising potential. These techniques are widely implement in optical design programs[29]. We will use a Zemax implementation of these techniques that combines local damped least squares routines with genetic algorithms[25].

2.4 Use of a commercial GRIN lens.

In order to test the accuracy and possibilities of the present methodology we tested the technique with a GRIN bi-convex commercial lens, GBX-25-40 (GRADIUM® LigthPath Technologies). This lens has a clear aperture of 22 mm, effective focal length 40 mm, thickness of 4.6 mm and has an axial gradient index with a complex profile described by an eleventh order power series polynomial. The profile is shown in Figure 3. This lens is a good test for the technique to be used with real crystalline lenses because the dimensions are similar, and most importantly, the profile is of sufficiently high complexity and number of parameters that it could represent real structures of the GRIN in real crystalline lens. Further, it is possible to obtain from the manufacturer the unique form of the eleventh order power series polynomial description of the gradient of

the lens. Since the profile depends only on the coordinates along the optic axis it is only necessary to do a 1-D laser scan in the sagittal plane. However the accuracy of the results can be extended to a 3-D scheme in the sense that a 2-D scan is simply composed of information from two identical orthogonal 1-D scans. The empirical scan of this lens was performed in a range of (-4, 4) mm at steps of 5 μm, i.e. using 1601 rays.

2.5 Construction of the merit function with a commercial GRIN.

To construct the merit function independent of the refracted rays slopes we used two constraints as described in section 2.1. To ensure a monotonically decreasing constraint in the profile, the derivate of **u** should be negative for all values of the optics axis coordinates. This condition must be expressed algebraically to be implemented in the merit function. This can be done by constraining all the roots of the second derivate of **u** (extreme values in first derivate) to be negative. However finding all possible roots of the eleventh order polynomial could result in an extremely large number of constraints. In order to reduce the number of operands in the merit function (the larger number of operands the slower the optimization routine) we forced the first derivate to be negative in an equally spaced number of points in the axis coordinate: [0 0.92 1.84 2.76 3.68 4.6] mm. As it will be shown in the results this is enough to force the monotonic constraint.

2.6 Relevance of the GRIN reconstruction in optical evaluation

To quantify the significance of the error in the GRIN reconstruction an analysis should be done to determine how this error is propagated to the wave aberration that characterizes the optical quality of the lens. Further, in practice these data could be used in comparison with data in the literature of global wave aberration of the human eye with aberroscopes or aberrations of the human cornea from corneal topography. As the GRADIUM lens has rotational symmetry, only spherical aberration is present on axis. To evaluate the error propagation influence for asymmetric aberrations we have

evaluated wave aberration off-axis (say 10º in the saggital plane) in terms of Zernike polynomial expansion.

3. Results

3.1 GRIN reconstruction.

Testing optimization routines

The accuracy of the optimization algorithms alone can be evaluated isolated from the experimental error in the empirical measurements. This is important to understand the maximum capabilities of the algorithm. This is accomplished by performing a virtual ray tracing, with Zemax, through the lens using the nominal parameters with the specific profile to evaluate the slopes of ray exiting the design lens. This information is then used as the "experimental data", supposing an unknown profile. Starting value for the parameters are chosen to give a linear profile for the GRIN in order to test the ability of the algorithm to reach a good solution when starting so far from the real profile. Figure 3 shows the nominal lens GRIN profile (black line), compared with retrieved with "free error" slope data (purple line). The mean absolute error is 0.0024±0.0022.

GRIN reconstruction from experimental data

The profile reconstructed using the real experimental slope data is also represented in Figure VIII.3 (purple line), for which the mean absolute error is 0.041±0.017.

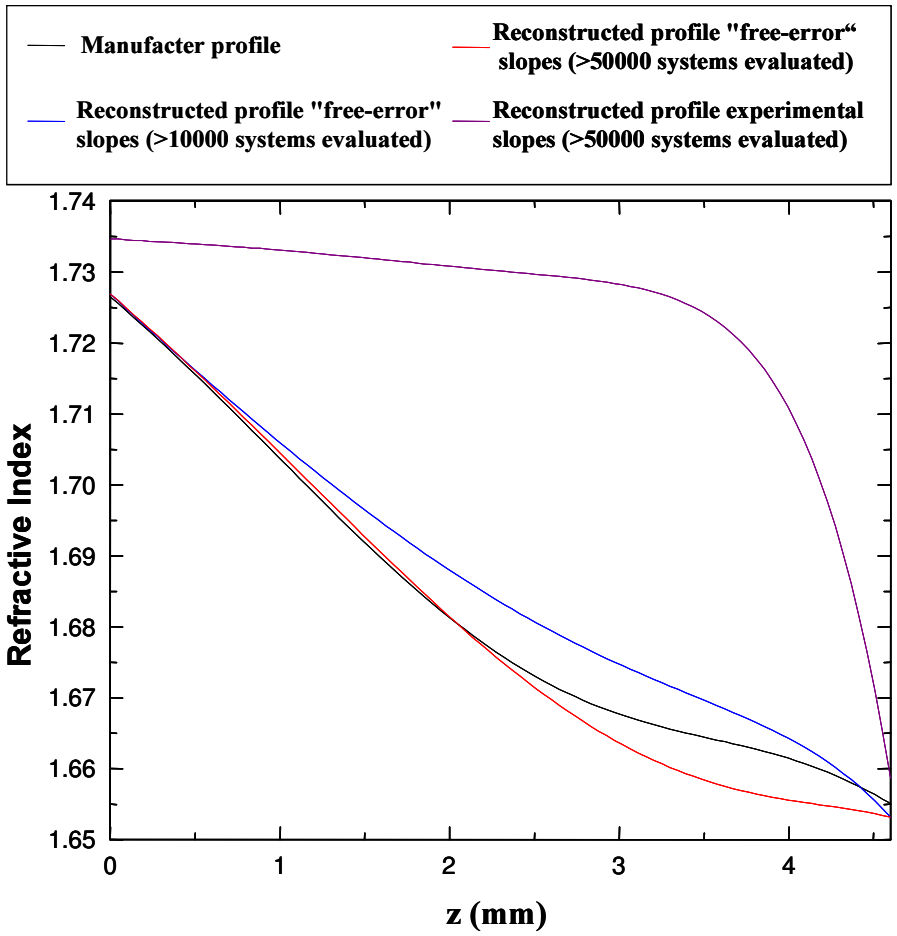

Figure VIII.3: Nominal lens profile given by the manufacter (black line) in comparison with reconstructed profiles. The number of systems evaluated indicates the number of different combinations used by the optimization routine. The blue line represents the reconstructed profile using error-free slopes with more than 10000 systems evaluated. The red line is the same, but for more than 50000 systems evaluated. The purple line represents the reconstructed profile using the real experimental data for more than 50000 systems.

3.2 Experimental accuracy

Figure VIII.4 shows the absolute errors in the slope measurements of deflected rays (the theoretical values from ray tracing of the manufacture data minus the scanning laser experimental measurements).

It should be noted that the distribution of errors is not random. There is an increasing error with increasing height of the entrance ray, and slightly higher variation in values corresponding to rays close to optical axis. This distribution of errors reveals that the experimental data tends to over-estimate the theoretical values. The root-mean square

error gives a global estimate of the error as being $7.231*10^{-4}$. It should be noted that the differences between the manufacturer lens data and the actual lens are considered negligible compared with the error in the slope measurements.

3.4 Relevance of the GRIN reconstruction in optical evaluation

Figure VIII.5 A, shows the wave aberration of the test lens (10º off-axis in the meridian plane) using the manufacturer profile (RMS of 0.7046 µm) and Figure 5 B&C show off axis wave aberrations of the manufacture profile minus the best reconstruction wave aberration for the GRIN –with simulated error-free experimental data (RMS of 0.7043 µm) and real experimental data (RMS of 0.7307 µm) respectively. These "difference" maps are referred as wave aberration residuals.

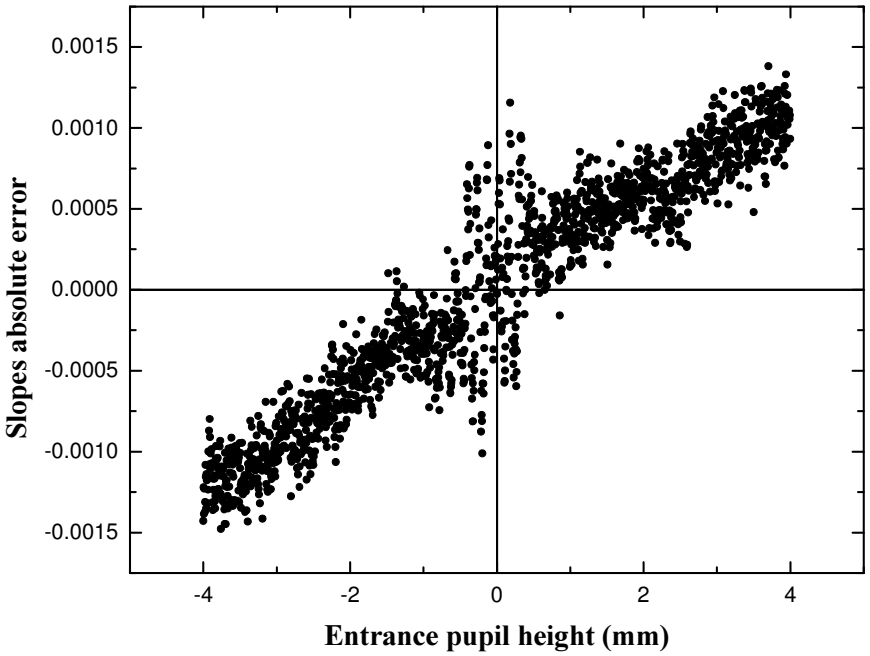

Figure VIII.4: Absolute errors in the slope measurements of deflected rays (the theoretical values from manufacture data minus the experimental measurements) as function of entrance pupil height position of the incoming ray.

The mean standard deviation error of Zernike coefficients has been frequently used in the literature to evaluate the experimental error sets of wave aberration measurements in the eye. It has been reported [30] that for a RMS global wave aberration of 0.5 µm the average standard deviation across Zernike coefficients in individual techniques is 0.071 µm (0.066 µm for a Hartmann-Shack sensor, 0.063 µm for a Laser ray tracing technique and 0.084 µm for Spatially resolved refractometer), while for corneal aberrations for a control eye (RMS 0.59 µm)–see chapter II- the Zernike coefficient average standard deviation is 0.016 µm.

With simulated error-free "experimental" data we obtained for the best reconstruction a mean standard deviation error of the Zernike coefficients of 0.00021 µm. Therefore the theoretical reconstruction of the GRIN results in an error in wave-front evaluation which is much lower than error in the experimental wavefront sensing techniques. However for the real experimental data the standard deviation increased to 0.014621 µm which was much higher and a similar order of magnitude as the error found in experimental wavefront sensing techniques.

It should be noted that in the GRADIUM lens we are evaluating the wave aberration in has an axial GRIN, and it is known that the influence on aberrations of changes in the GRIN structure are different for a radial GRIN [23]. It is expected that the amount of error in wave aberration estimation in a radial or mixed GRIN could change the amount of the error.

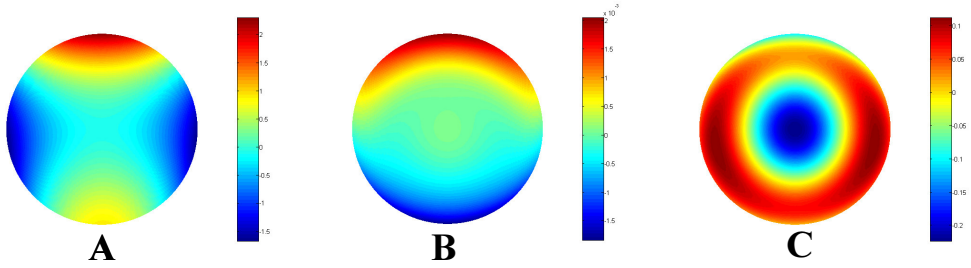

Figure VIII.5: A) The wave aberration using the manufacturer profile. Colorbar scale from -1.5 µm to 2 µm. **B)** Subtraction of the wave aberration of the manufacter profile minus the free-error experimental reconstructed profile. Colorbar scale from -0.0015 µm to 0.002 µm. **C)** Subtraction of the wave aberration of the manufacter profile minus the real experimental reconstructed profile. Colorbar scale from -0.2 µm to 0.1 µm.

4. Discussion

4.1 Sources and implications of experimental errors.

Previous works have analyzed the effect of errors in experimental deflectometry data on the mathematical algorithms to reconstruct GRIN profiles assuming a Gaussian distribution of the experimental errors [17, 31]. However as it is shown in section 3.2 the more common situation is that experimental error is more likely to have a systematic rather than a random distribution, and hence the influence over the reconstruction would be different. Previous authors [12] fitted experimental data of refracted rays to analytic functions, hence smoothing raw data. This may smooth experimental dispersion errors but would not correct a systematic error such as an over-estimation.

There are several factors that could explain the sources of experimental errors:

1) Firstly in the actual configuration we assume that differences between the lens design and the actual lens are negligible compared with experimental errors, although it appears to be a reasonable assumption considering low tolerance values of the manufactured lens.

2) Errors in centration of the lens. Because the method to assess the centration uses the same optical set-up some degree of error it is expected.

3) The resolution of the camera –the number of pixels used per mm- depends on the number of pixels of the CCD (512x480) and the magnification of the optics of the camera.

4) Optics of the camera objective. The objective of the camera could introduce some systematic errors due to its optical aberrations. For example the general tendency in the over-estimation of the slopes could be produced by distortions in the focusing objective.

There is a compromise solution between 3) and 4). On one hand, resolution increases by moving the GRIN lens closer to the camera. On the other hand, aberrations of the camera lens increase as the object is moved closer to the camera and also there is a decrease in the field of view and of the ray path to analyze.

5) Image processing techniques. Apart of image processing with Optimas as described in section 2.2 we developed an alternative code written in Matlab using a threslholding pre-processing algorithm and using built-in "edge" functions written in Matlab Image Processing Toolbox (Version 3.1(R.12.1)). The maximum difference in the two methods of computing the slopes is 0.0005, thus implying that at least the image processing is not introducing a significant or systematic slope error.

In the present work, the errors of evaluating surfaces shapes by image processing has not been evaluated. It would be possible to undertake this analysis to understand the impact of that source of error in this approach, and it is clear that it would play a role in the accuracy of the final solution. This would be particularly applicable to the surface profiles of physiological lenses which might be expected to have asymmetries.

4.2 Possibilities of the extension through a 3-D GRIN reconstruction

Although the present analysis has been developed for a 2-D scheme it is straightforward to extend it to 3-D, where ray directions are evaluated in 2-D, from each of the two cameras, one from above and the other from the side.

In the empirical realization of this approach to understand the GRIN structure of a physiological lens, the problem of still not knowing with certainty details of the proper functional GRIN model for the physiological lens still remains. More complex and more realistic functional models for the GRIN inside the lens should be proposed from those actually used. Such models must be necessarily be based on data from physiological measurements and also should consider that two of the classical assumptions in lens modelling, namely iso-indical concentric surfaces and rotationally symmetry are not strictly valid [20].

5. Conclusions and future tasks

Actual methods to reconstructed GRIN structure in the crystalline lens present some limitations because of the experimental procedure, in destructive techniques, and the

limitations in the mathematical algorithms and errors in experimental data in tomography methods. We have presented a variant of a tomography method showing global optimization to be a robust procedure even with models employing a large number of parameters in absence of experimental errors. However in the real case of using the real experimental data the error in the reconstruction increase significantly due to the *ill-conditioned* nature of the optimization in such case. In addition we have shown how the errors in the reconstruction of the GRIN is propagated to the estimation of the wave aberration of the test GRIN lens. Future prospects following this work include:

1) Try to avoid the experimental errors in slope measurements by correcting the optics of the experimental set-up, in the camera objective and optimizing the set-up configuration.

2) Study and evaluate he effect of surface shape measurement and its errors in the GRIN reconstruction.

3) Optimize the time used by the optimization routines.

4) Advance in the development of realistic models for the GRIN structure of the crystalline lens.

The final goal is to use the present technique in the measurement of real crystalline lens GRIN, with a known accuracy and range of errors.

6. References

1. M. C. W. Campbell and A. Hughes, "An analytic, gradient index schematic lens and eye for the rat which predicts aberrations for finite pupils," Vision Res 21, 1129-1148 (1981).
2. A. Roorda, "Human visual system - Image formation," in *Encyclopedia of imaging science and technology*, J. P, ed. (John Wiley & Sons, New York, 2002), pp. 539-557.
3. B. K. Pierscionek, G. Smith, and R. C. Augusteyn, "The refractive increments of bovine a-, ß-, and g-crystallins," Vision Res 27(9), 1539-1541 (1987).
4. G. Smith, B. K. Pierscionek, and D. A. Atchison, "The optical modelling of the human lens," Ophthal Physiol Opt 11, 359-369 (1991).
5. D. A. Palmer and J. Sivak, "Crystalline lens dispersion," J Opt Soc Am A 71, 780-782 (1981).
6. S. Nakao and S. Fujimoto, "Model of refractive index distribution in the rabbit crystalline lens," J Opt Soc Am A 58(8), 1125-1130 (1968).
7. P. P. Fagerholm, B. T. Philipson, and B. Lindstrom, "Normal human lens-distribution of protein," Exp Eye Res 33, 615-620 (1981).

8. B. A. Moffat, D. A. Atchison, and J. M. Pope, "Age-related changes in refractive index distribution and power of the human lens as measured by magnetic resonance micro-imaging in vitro," Vision Res 42, 1683-1693 (2002).

9. O. Pomerantzeff, M. M. Pankratov, G. J. Wang, and P. Dufault, "Wide-angle optical model of the eye," Am J Optom Physiol Opt 61, 166-176 (1984).

10. J. H. Al-Ahdali and M. A. El-Messiery, "Examination of the effect of the fibrous structure of a lens on the optical-characteristics of the human eye:a computer simulated model," Appl Opt 34, 5738 (1995).

11. E. H. Roth and G. Kluxen, "In vivo measurements of the distribution of the refractive index of the human lens with a Scheimpflug's procedure on the anterior segment of the eye and a He-Ne laser beam," Fort Ophthalmol 87, 312-316 (1990).

12. M. C. W. Campbell, "Measurement of refractive index in an intact crystalline lens," Vision Res 24, 409 (1984).

13. D. Y. C. Chan, J. P. Ennis, B. K. Pierscionek, and G. Smith, "Determination and modelling of the 3-D gradient refractive indices in crystalline lens," Appl Opt 27, 926-931 (1988).

14. L. F. Garner, G. Smith, S. Yao, and R. C. Augusteyn, "Gradient refractive index of the crystalline lens of the Black Oreo Dory (Allocyttus Niger): comparison of magnetic resonance imaging (MRI) and laser ray-trace methods," Vision Res 41, 973-979 (2001).

15. P. L. Chu, "Nondestructive measurements of index profile of an optical-fibre prefrom," Electron. Lett. 12, 136 (1977).

16. E. Acosta, R. Flores, D. Vázquez, S. Ríos, L. F. Garner, and G. Smith, "Tomographic method for measurement of the refractive index profile of optical fibre preforms and rod GRIN lenses," Jpn J Appl Phys 41, 4821-4824 (2002).

17. G. Beliakov and D. Y. C. Chan, "Analysis of inhomogeneous optical systems by the use of ray tracing. I. Planar systems," Appl Opt 36(22), 5303-5309 (1997).

18. G. Beliakov and D. Y. C. Chan, "Analysis of inhomogeneus optical systems by the use of ray tracing. II. Three-dimensional systems with symmetry," Appl Opt 37, 5106-5111 (1998).

19. W. H. Press, S. A. Teukolsky, W. T. Vetterling, and B. P. Flannery, *Numerical recipes in C: The art of scientific computing,* 2 ed. (Cambridge University Press, 1992).

20. B. K. Pierscionek, "Refractive index contours in the human lens," Exp Eye Res 64, 887-893 (1997).

21. A. Glasser and M. Campbell, "Presbyopia and the optical changes in the human crystalline lens with age," Vision Research 38(2), 209-229 (1998).

22. A. Glasser and M. Campbell, "Biometric, optical and physical changes in the isolated human crystalline lens with age in relation to presbyopia," Vis. Res. 39, 1991-2015 (1999).

23. D. J. Fischer, "Gradient-index ophthalmic lens design and polymer material studies," (University of Rochester, Rochester, New York, 2002).

24. D. V. Sharma, D. K. Shumar, and A. K. Ghatak, "Tracing rays through graded index media," Appl Opt 21, 984-987 (1982).

25. K. E. Moore, "Algorithm for global optimization of optical systems based upon genetic competition," presented at the Optical design and analysis software, Denver, Colorado, 1999.

26. J. Meiron, "Damped least-squares method for automatic lens design," J Opt Soc Am A 55(9), 1105-1109 (1965).

27. K. D. Kihm, S. Okamoto, D. Tsuru, and H. S. Ko, "Adoption of a genetic algorithm (GA) for tomographic reconstruction of line-of-sight optical images," Experiments in Fluids 22, 137-143 (1996).

28. K. D. Kihm and D. P. Lyons, "Optical tomography using a genetic algorithm," Opt Lett 21(17), 1327-1329 (1996).

29. D. Vasiljevic, "Program for optical system design and optimization," (2002).

30. E. Moreno-Barriuso, S. Marcos, R. Navarro, and S. Burns, "Comparing Laser Ray Tracing, Spatially Resolved Refractometer and Hartmann-Shack Sensor to measure the ocular wave aberration," Optom Vis Sci 78, 152-156 (2001).

31. M. A. R. Rama, S. Acosta, E., "New treatment for tomographic reconstruction of refractive index profiles of inhomogeneous objects from slope measurements," Jpn. J. Appl. Phys. 37, 3682-3685 (1998).